

1 **Gut microbiome is associated with recurrence-free survival in patients with resected**
2 **Stage IIIB-D or Stage IV melanoma treated with immune checkpoint inhibitors**

3
4 Mykhaylo Usyk¹, Richard B. Hayes^{1,2}, Rob Knight³, Antonio Gonzalez³, Huilin Li^{1,2}, Iman
5 Osman^{2,4,5}, Jeffrey S. Weber^{2,5} & Jiyoun Ahn^{1,2,#}

6
7
8 ¹ Department of Population Health, NYU Grossman School of Medicine, New York, NY, USA

9 ² NYU Laura and Isaac Perlmutter Cancer Center, New York, NY, USA

10 ³ Departments of Pediatrics, Computer Science & Engineering, and Bioengineering; Center for
11 Microbiome Innovation, University of California, San Diego, La Jolla, CA

12 ⁴ The Ronald O. Perelman Department of Dermatology, NYU Grossman School of Medicine,
13 New York, NY, USA

14 ⁵ Department of Medicine, NYU Grossman School of Medicine, New York, NY, USA

15
16 # Corresponding author email: Jiyoun.Ahn@nyulangone.org

17
18
19 **Conflict of Interest Disclosures:** The authors declare no potential conflicts of interest

20
21 **Funding/Support:**

22 Research reported in this publication was supported in part by the U.S. National Cancer Institute
23 under award numbers P50 CA225450, P20CA252728, P30CA016087, R01CA159036,
24 R01LM014085-01A1, and U01CA250186.

25
26

27

28 **Highlights**

29

- 30 • Overall gut microbiome (GMB) composition is largely unchanged during ICB treatment.
- 31 • GMB composition varies by geographic region
- 32 • We identified gut bacterial markers associated with recurrence in region-specific analyses.
- 33 • Region-identified markers are generalizable if GMB composition is taken into account
- 34 by matching.

35

36

37 **Summary (150 Words)**

38

39 The gut microbiome (GMB) has been associated with outcomes of immune checkpoint blockade
40 therapy in melanoma, but there is limited consensus on the specific taxa involved, particularly
41 across different geographic regions. We analyzed pre-treatment stool samples from 674
42 melanoma patients participating in a phase-III trial of adjuvant nivolumab plus ipilimumab versus
43 nivolumab, across three continents and five regions. Longitudinal analysis revealed that GMB
44 was largely unchanged following treatment, offering promise for lasting GMB-based
45 interventions. In region-specific and cross-region meta-analyses, we identified pre-treatment
46 taxonomic markers associated with recurrence, including *Eubacterium*, *Ruminococcus*,
47 *Firmicutes*, and *Clostridium*. Recurrence prediction by these markers was best achieved across
48 regions by matching participants on GMB compositional similarity between the intra-regional
49 discovery and external validation sets. AUCs for prediction ranged from 0.83-0.94 (depending
50 on the initial discovery region) for patients closely matched on GMB composition (e.g., JSD
51 ≤ 0.11). This evidence indicates that taxonomic markers for prediction of recurrence are
52 generalizable across regions, for individuals of similar GMB composition.

53

54

55 Introduction

56
57 Melanoma is the 6th most common form of cancer in the U.S., accounting for approximately
58 100,000 new cases annually (Siegel et al., 2023). Immune checkpoint blockade (ICB), utilizing
59 monoclonal antibodies targeting programmed death 1 (PD-1) and cytotoxic T-lymphocyte
60 antigen 4 (CTLA-4), are treatment options that can provide durable benefit in metastatic and
61 high-risk resected melanoma. However the benefit of ICB is unpredictable and 25-30% of those
62 treated experience cancer recurrence (Weber et al., 2023). Identifying robust biomarkers to
63 predict treatment outcomes is imperative. Predictive markers may support personalized
64 treatment plans, resulting in improved patient management, ultimately enhancing treatment
65 efficacy and outcomes.

66
67 Accumulating evidence suggests that the gut microbiome (GMB) influences survival,
68 progression and recurrence in ICB-treated melanoma (Gopalakrishnan et al., 2018; Matson et
69 al., 2018; Routy et al., 2018; Peters et al., 2019). These associations have been further
70 supported by intervention experiments, in clinical trials and animal models, which have
71 demonstrated the potential for improved outcomes in melanoma through fecal microbiome
72 transplant (FMT) (Baruch et al., 2021; Davar et al., 2021; McQuade et al., 2020). Notably,
73 clinical trials conducted by Davar *et al.* (Davar et al., 2021) and Baruch *et al.* (Baruch et al.,
74 2021) showed evidence of ICB response in treatment-refractory patients following FMT,
75 associated with consistent activation of CD8⁺ T cells. Additionally, several pre-clinical human-
76 to-mouse FMT transplant studies demonstrated similar T-cell activity in anti-PD-L1-based
77 therapies for melanoma (Gopalakrishnan et al., 2018; Matson et al., 2018). Furthermore, studies
78 showed that a high-fiber diet in melanoma patients undergoing ICB in the neoadjuvant setting
79 was related to alteration in GMB and enhanced treatment response (Simpson et al., 2022), with
80 further confirmation in a pre-clinical mouse model where high-fiber treatment was associated
81 with changes in the GMB and improved treatment outcomes (Spencer et al., 2021).

82
83 Although these studies provide promising clinical insights, the identified bacterial markers for
84 predicting treatment outcomes in melanoma have varied considerably among studies (Lee et
85 al., 2022). In fact, in a recent multi-regional analysis of European patients, Lee *et al.* argued that
86 GMB markers are region specific (Lee et al., 2022). While this discrepancy in bacterial marker
87 identification, by region, may be attributed to clinical selection criteria, different ICB treatment
88 modalities, small sample sizes, or population-specific characteristics (He et al., 2018b; Lee et
89 al., 2022), it is becoming evident that geographic variation in compositional attributes likely plays
90 an important role (Lee et al., 2022), as geography, as well as relocation, are known to be strong
91 determinants of GMB composition (He et al., 2018b; Kaplan et al., 2019; Peters et al., 2020;
92 Vangay et al., 2018). This underscores the critical need to sample the microbiome from diverse
93 patient groups and geographic areas to comprehensively capture GMB biodiversity and identify
94 robust bacterial markers for treatment outcomes and their associated contexts.

95
96 For the current investigation, we studied participants in the Checkmate 915 randomized, double-
97 blind, phase III trial (ID: NCT02388906), that was composed of 1,833 patients who received
98 nivolumab 240 mg once every 2 weeks plus ipilimumab 1 mg/kg once every 6 weeks (916
99 patients) or nivolumab 480 mg once every 4 weeks (917 patients) for \leq 1 year. In this cohort, we
100 investigated the association between GMB and melanoma recurrence in 674 trial participants
101 who provided stool samples. This study was carried out under a standard protocol across five
102 broad geographic regions, allowing for a detailed analysis of the regional association of GMB
103 with treatment outcomes and allowing us to directly address the issue of geographic variation
104 while maximizing bias control via rigorous clinical trial design. In pre-treatment stool samples
using shotgun metagenomics, we achieved strain-level resolution of the GMB. We demonstrate

105 broad generalizability of certain strains of bacteria in meta-analysis and more robust cross-
106 regional prediction, overcoming previous replication hurdles, via GMB matching. Additionally,
107 we sequenced stool samples collected at 7 weeks and 29 weeks after treatment initiation in a
108 sub-sample, to assess the stability of the GMB following ICB treatment. This investigation is the
109 first to explore the GMB in melanoma patients in the adjuvant setting, potentially uncovering
110 crucial insights that could lead to more effective, personalized treatment strategies to improve
111 patient outcomes.

112 Results

113

114 Patient Characteristics

115 Our prospective study of GMB and melanoma included 674 patients with resected stage IIIB-D
116 or IV melanoma, who were randomized to receive adjuvant nivolumab plus ipilimumab or
117 nivolumab alone (Weber et al., 2023). All participants provided a stool sample prior to ICB
118 treatment and approximately half of the patients provided stool samples post-treatment (at
119 weeks 7 and 29 follow-up visits) (**Supplemental Figure 1**). The 674 patients were evenly
120 distributed between the combination therapy and nivolumab monotherapy arms (**Table 1**).
121 Patients were majority white (99.0%) and male (58.9%), and the mean (SD) age was 55.0 (13.9)
122 years. Melanoma recurrence was similar for the combination (35.0%) and nivolumab arms
123 (39.8%), similar to what was previously reported for the full trial series (35.4% vs. 36.8%)(Weber
124 et al., 2023).

125 Global beta diversity analysis using Jensen-Shannon divergence (JSD, a measure of GMB
126 similarity between pairs of samples) revealed that GMB differed significantly by region, sex,
127 stage, and gender, both when performing univariate and co-adjusted analyses (**Figure 1A**).
128 The gut microbiome compositions from North American (USA and Canada) and Eastern
129 European participants showed the greatest pairwise dissimilarity ($R^2=4.84\%$, $p=0.001$), while
130 those from Eastern and Western European participants, the two most proximal areas, showed
131 minimal differences (PERMANOVA $R^2 = 0.52\%$, $p\text{-value}=0.034$ (**Figure 1B**).

132 GMB and Recurrence

133 GMB structure (beta diversity) was not associated with melanoma recurrence in the overall
134 study of 674 patients (in both crude and adjusted analysis, **Figure 1A**). These relationships
135 were similar for the two arms of the trial ($R^2=0.003$, $p\text{-value}=0.67$ and $R^2=0.003$, $p\text{-value}=0.38$,
136 PERMANOVA for combination and mono treatment respectively). In region-stratified analysis,
137 GMB beta diversity was associated with recurrence in North America ($R^2=0.022$, $p\text{-}$
138 $\text{value}=0.023$), Western Europe ($R^2=0.005$, $p\text{-value}=0.049$) and rest of world (Brazil and New
139 Zealand) (ROW) ($R^2=0.07$, $p\text{-value}=0.007$); there was no evidence of association for Australia
140 ($R^2=0.009$, $p\text{-value}=0.32$) or Eastern Europe ($R^2=0.027$, $p\text{-value}=0.36$) (**Figure 1C-G**). Because
141 of the differential GMB associations by geographic regions, subsequent analyses are based on
142 region-specific analyses.

143

144 In region stratified analyses using ANCOM-BC, we identified several GMB taxa associated with
145 recurrence. Nine bacterial taxa were associated with recurrence in North America (**Figure 2A** -
146 dark green points and **Supplemental Table 1**): *Eubacterium* sp. CAG:115, *Ruminococcus* sp.
147 CAG:177, *Eubacterium* sp. CAG:786, *Eubacterium siraeum*, *Firmicutes bacterium* CAG:137,
148 *Clostridium* sp. CAG:780, *Clostridiales bacterium* 1-7-47, *Firmicutes bacterium* CAG:884,
149 *Aeromonas salmonicida*, and *Peptostreptococcus anaerobius*. Among these, bacteria belonging
150 to the genera of *Eubacterium*, *Ruminococcus*, *Firmicutes*, and *Clostridium* have previously been
151 identified as predictive of recurrence in melanoma (Lee et al., 2022; Matson et al., 2018; Routy
152 et al., 2018), while *Aeromonas salmonicida* and *Peptostreptococcus anaerobius* represent novel
153 markers. In Western Europe (**Figure 2A** - brown points), two novel markers, *Bariatricus*
154 *massiliensis* and *Blautia schinkii*, were identified. In ROW we identified a *Clostridium*,
155 *Clostridiales bacterium* 1-7-47FAA, while for Eastern Europe, *Lawsonia intracellularis*, a novel
156 marker, was the only recurrence-associated taxa identified.

157

158 We performed a meta-analysis on these region-specific markers across all regions, to determine
159 whether the markers associated with recurrence in one region were generalizable. Although
160 there is significant heterogeneity between regions, we found that seven regionally identified

161 recurrence markers were also associated with recurrence in cross-region meta-analyses
162 (**Figure 2B-K**), including markers initially identified for North America (*Eubacterium* sp.
163 *CAG:115*, *Ruminococcus* sp. *CAG:177*, *Eubacterium* sp. *CAG:786*, *Eubacterium siraeum*),
164 Western Europe (*Bariatricus massiliensis* and *Blautia schinkii*), and Eastern Europe (*Lawsonia*
165 *intracellularis*). In meta-analyses excluding the original discovery region, *Eubacterium* sp.
166 *CAG:115* and *Eubacterium* sp. *CAG:786* remained significantly associated in the same
167 (protective) direction, indicating the potential role of these bacteria in a general context, while
168 *Ruminococcus* sp. *CAG:177*, *Bariatricus massiliensis* and *Blautia schinkii* remained significant,
169 but showed an inverse association (**Figure 2B-K**, bottom common effect shown in red). This
170 suggested a potential GMB context specificity of taxonomic markers for recurrence; that is,
171 specific GMB markers may predict recurrence given a specific GMB composition. This is
172 explored in “*GMB matching facilitates cross-regional generalizability*” section below.
173

174 To explore the potential functional mechanisms of microbial association with recurrence, we
175 investigated the association between recurrence-associated taxa, from region-stratified
176 analyses (see **Figure 2A**), and KEGG Level 3 pathways. We identified 57 functional pathways
177 linked to recurrence-associated species (FDR <0.0001) (**Figure 3A**). Fifty-five of the 57
178 pathways were classified as “Metabolism” at KEGG Level 1, with the remaining two are involved
179 in the biosynthesis of secondary metabolites. Given prior findings illustrating a connection
180 between fiber consumption, gut microbiota shifts, and improved melanoma outcomes during
181 treatment (Spencer et al., 2021), we focused on 15 carbohydrate-associated “Metabolism”
182 pathways with correlations >0.3, including for amino-sugar and nucleotide-sugar metabolism
183 (**Figure 3B**). Of the 15 carbohydrate-associated pathways, 8 were differentially associated with
184 recurrence in the North American region, but not in other regions (FDR<0.0001, adjusted for
185 age, sex, tumor stage, BRAF mutation and study arm) (**Figure 3C**).
186

187 *GMB matching facilitates cross-regional generalizability*

188 Regional GMB heterogeneity is a major barrier to the development of reliable gut microbial
189 markers for melanoma outcomes (He et al., 2018a). Recognizing this, we then tested whether
190 recurrence-associated bacteria (**Figure 2A**) exhibited stronger prediction for recurrence in
191 individuals selected for closely similar overall GMB composition (JSD distance), regardless of
192 geographic region (**Figure 4A**). The prediction of recurrence in non-North American
193 participants related to the North America-specific markers (**Figure 2A**) was strongest for those
194 most closely matched to the North Americans on JSD distance (**Figure 4B**). Non-North
195 American participants matching North American participants at JSD of ≤ 0.11 (n=61) showed an
196 AUC of 0.88. Furthermore the AUC was highly inversely correlated to JSD similarity (correlation
197 = -0.85, p<0.001), indicating that the smaller the beta-diversity distance between matched pairs,
198 the stronger the prediction was in non-North American (validation set) participants of markers
199 initially identified in North Americans (discovery set). Similar relationships were observed for
200 markers initially identified in Western Europe (**Figure 4C**), Eastern Europe (**Figure 4D**), and
201 ROW (rest of the world) (**Figure 4E**), with the strongest predictions among those most closely
202 matched on JSD (e.g., JSD ≤ 0.11). Similar results are found for other measures of beta
203 diversity (**Figure 4F**). While there were differences in number of patients retained using
204 different beta-diversity measures (**Figure 4F**), the overall pattern was the same and consistently
205 indicated that close GMB matching, regardless of distance metric choice, yielded more robust
206 generalizability.
207

208 *Temporal Stability of GMB Following ICB Treatment*

209 To assess the temporal stability of the GMB, we calculated intra-patient microbial JSD distances
210 at baseline, week 7, and week 29, in 248 study participants with available serial stool samples,
211 and as a comparison, we also calculated the unpaired inter-patient JSD distances (**Figure 4**). In

212 this analysis, JSD values close to 0 indicate similarity, while JSD close to 1 indicate dissimilarity.
213 We found that the GMB for individuals remained consistent across visits (global PERMANOVA
214 across all three time-points, $R^2 = 0.867$, p -value < 0.001), with remarkable stability of the GMB
215 from before (baseline) and during (7 and 29 weeks) ICB therapy. The findings are consistent for
216 oth treatment arms (nivolumab plus ipilimumab combination: $R^2 = 0.852$, $p < 0.001$ and
217 nivolumab only $R^2 = 0.902$, $p < 0.001$) (see **Supplementary Figure 2**). Analysis of time-points as
218 the outcome in place of patients did not reveal any significant compositional differences
219 (**Supplemental Figure 4**), indicating that treatment did not have a targeted effect on the GMB
220 ($R^2 = 0.0019$, p -value=0.76). Longitudinal samples were more likely to be provided by those
221 who didn't experience recurrence during the trial (see **Supplemental Table 2**; recurrence rate:
222 27.2% for those providing longitudinal samples vs. 44.8% for those who didn't). However,
223 among those who provided samples, the GMB remained stable regardless of recurrence status
224 (see **Supplement Figure 3**). GMB composition thus remained predominantly unchanged post-
225 treatment without any identifiably consistent temporal shifts due to treatment, although a modest
226 destabilization was noted for the combination treatment compared to the mono-treatment arm.
227
228
229

230 Discussion

231
232 We investigated associations of the gut microbiome with melanoma recurrence, in the multi-
233 center Checkmate 915 phase III trial of adjuvant immune checkpoint blockade (ICB), with
234 nivolumab plus ipilimumab or nivolumab alone (Weber et al., 2023). We found that melanoma
235 recurrence was associated with gut microbial taxa from the *Eubacterium*, *Ruminococcus*,
236 *Firmicutes*, and *Clostridium* genera in region-specific and cross-region meta-analyses.
237 Recurrence prediction by these markers was best achieved across regions by matching on
238 GMB compositional similarity between the intra-regional discovery and external validation sets.
239 AUCs for prediction ranged from 0.83-0.94 (depending on the initial discovery region), for
240 patients closely matched on GMB composition (e.g., JSD ≤ 0.11). This evidence indicates that
241 taxonomic markers for prediction of recurrence are generalizable across regions, for individuals
242 of similar GMB composition. Lastly, we examined longitudinal samples from patients during
243 treatment and discovered that the GMB composition remained largely constant over the
244 treatment period, indicating stability of the gut microbiome throughout the ICB treatment course.

245
246 We identified specific bacterial strains that predict recurrence in the adjuvant setting. The
247 *Eubacterium*, *Ruminococcus*, *Firmicutes*, and *Clostridium* have been previously associated with
248 outcomes for ICB in the metastatic setting (Lee et al., 2022; Matson et al., 2018; Routy et al.,
249 2018). *Eubacterium* has been shown to modulate the efficacy of immunotherapies, by promoting
250 an anti-inflammatory environment via natural killer cell interaction (Liu et al., 2023). Similarly,
251 *Clostridium* and *Firmicutes* have been linked to enhanced immunoregulatory responses, related
252 to modification of the T-cell response which may directly enhance the effects of immunotherapy
253 (Shim et al., 2023). *Ruminococcus*, on the other hand, has been associated with both pro- and
254 anti-inflammatory effects, particularly related to increases in CD4+ and CD8+ T cells, potentially
255 influencing the outcomes of immune checkpoint therapies (Araji et al., 2022). Additional
256 recurrence-associated taxa identified in this study include *Lawsonia*, *Bariatricus*, and *Blautia*,
257 the latter of which was also associated with ICB treatment outcomes in our previous pilot
258 research (Peters et al., 2019). The results shown here in the adjuvant setting and research in
259 the metastatic setting (Lee et al., 2022; Matson et al., 2018; Routy et al., 2018) (Peters et al.,
260 2019) are beginning to identify bacteria that impact ICB treatment outcomes, setting the stage
261 for future studies modifying the GMB to achieve more favorable outcomes in a variety of ICB
262 contexts.

263
264 Our analysis also showed connections between these immunomodulatory bacterial taxa and
265 carbohydrate metabolism pathways within the GMB, with associations related to glucose
266 metabolism being among the most numerous category. We observed significant correlations
267 between certain bacterial taxa, such as *Eubacterium* and *Ruminococcus*, and the KEGG Level 3
268 pathways related to carbohydrate metabolism. This is notable because
269 "glycolysis/gluconeogenesis" and "pentose phosphate pathway" have been related to both the
270 microbiome and cancer treatment success (Cullin et al., 2021). Similar findings have been
271 reported by Spencer et al (Spencer et al., 2021) who reported that dietary fiber can modulate
272 the gut microbiome (specifically *Eubacterium* and *Ruminococcus*) and enhance the response to
273 melanoma immunotherapy, implying that a high-fiber diet could shift the microbiome towards a
274 composition conducive to enhanced immunotherapy response. Previous evidence (Spencer et
275 al., 2021) along with our comprehensive study focusing on the adjuvant setting adds weight to
276 the proposition that dietary interventions on the GMB are a potential strategy to reduce
277 melanoma recurrence risk.

278
279 A barrier to progress in use of GMB biomarkers as tools for clinical prediction in ICB treatment
280 of melanoma is that GMB markers associated with melanoma outcomes tend to be population

281 specific (Lee et al., 2022), as geographic locality is a strong determinant of GMB composition
282 (Peters et al., 2020). In our study, we also observed significant variation in GMB composition
283 between regions internationally. We showed, however, that the capacity to predict recurrence
284 may be improved by limiting comparisons to subjects closely matched for GMB beta-diversity.
285 This implies, for practical application in the clinical setting, that prediction of recurrence for
286 individual melanoma patients may be achievable by comparison to referent data for patients
287 closely matched on GMB; this will require larger data sets well-characterized for GMB and ICB
288 outcomes than are currently available.

289
290 In our study, an important design element included sampling of the GMB before and at several
291 times during treatment, to assess ICB treatment-related changes in microbiome composition.
292 While in free-living populations, GMB remains highly stable over a time course that may span
293 years (Chen et al., 2021; Olsson et al., 2022), ours is the first study to demonstrate temporal
294 stability of the GMB in ICB-treated patients. Given previously reported improvement in
295 outcomes in ICB-treated melanoma patients by fecal microbiome transplant (FMT) (Derosa and
296 Zitvogel, 2021), our results suggest that FMT or other GMB modifiers could exert a stable
297 benefit throughout the treatment course. The stability of the GMB during ICB treatment, as
298 illustrated in our data, hints at its potential as a lasting therapeutic reservoir which by
299 alteration—whether through dietary changes, probiotics, or FMT—may offer a novel strategy for
300 enhancing the effectiveness of adjuvant ICB treatment.
301

302 **Methods**

303

304 **Study Population and Design**

305 Our gut microbiome study was based on the phase III CheckMate 915 trial (ID:
306 NCT02388906)(Weber et al., 2023), which originally evaluated adjuvant nivolumab plus
307 ipilimumab versus nivolumab alone in patients with resected stage IIIB-D or IV melanoma. The
308 primary endpoint was recurrence-free survival (RFS). The original trial reported that there was
309 no significant difference between treatment groups for RFS. For a full description of original trial
310 including outcome assessment and sample collection, refer to the original design publication
311 (Weber et al., 2023). Our prospective, analysis focused on a total of 674 patients who provided
312 a stool sample prior to treatment initiation (**Supplemental Figure 1**).

313

314 **Sample Collection and Sequencing**

315 Participants had the option to provide stool samples prior to the commencement of their
316 treatment. The ancillary microbiome study showed no significant differences compared to the
317 original trial in clinical and demographic variables (Weber et al., 2023). Participants average age
318 was 55 years. Most patients were stage IIIC, with a slightly higher proportion of men than
319 women. In order to quantify the impact of treatment on GMB, during and after treatment,
320 approximately half of the participants were also required to submit stool samples during their
321 treatment (specifically at week 7) and post-treatment (at week 29). The stool samples have
322 been collected using OMNIgene GUT kits (DNA Gentotek, Ontario, CA), which provide room
323 temperature stability of microbiome profiles for 2 months. All samples have been collected
324 during doctor visits and mailed by the patient to a centralized laboratory, per region, for storage
325 where samples were immediately store at -80°C .

326

327 These samples underwent rigorous shotgun metagenomics sequencing in the Knight laboratory
328 at the University of California San Diego (UCSD) as previously described (Usyk et al., 2023),
329 enabling us to achieve strain-level resolution of the GMB. DNA was extracted from stool
330 following the Earth Microbiome Project protocol (Thompson et al., 2017). Input DNA was
331 quantified, using a PicoGreen fluorescence assay (ThermoFisher, Inc), and normalized to 1 ng,
332 using an Echo 550 acoustic liquid-handling robot (Labcyte, Inc). Enzyme mixes for
333 fragmentation, end repair and A-tailing, ligation, and PCR were added using a Mosquito HV
334 micro pipetting robot (TTP Labtech). Fragmentation was performed at 37°C for 10 min, followed
335 by end-repair and A-tailing at 65°C for 30 min. Sequencing adapters and barcode indices were
336 added in two steps, following the iTru adapter protocol(Glenn et al., 2019). Universal “stub”
337 adapter molecules and ligase mix were first added to the end-repaired DNA using the Mosquito
338 HV robot and ligation performed at 20°C for 1 h. Unligated adapters and adapter dimers were
339 removed using AMPure XP magnetic beads and a BlueCat purification robot (BlueCat Bio).
340 Next, adapter-ligated samples were added to a 384-PCR plate containing unique i7 and i5 index
341 primers and PCR master mix, then PCR-amplified for 15 cycles. The amplified and indexed
342 libraries were purified again using magnetic beads and the BlueCat robot, re-suspended in
343 water, and transferred to a 384-well plate using the Mosquito HTS liquid-handling robot for
344 library quantitation, sequencing, and storage. Samples were normalized and pooled based on a
345 PicoGreen fluorescence assay, PCR cleaned, and size-selected on a PippinHT before
346 sequencing on an Illumina NovaSeq 6000 (S4 flow cell and 2x150bp chemistry) at the Institute
347 for Genomic Medicine at UCSD.

348

349

350 **Statistical and Bioinformatics Analysis**

351 GMB composition was determined in samples by using the woltka pipeline with the wolR1
352 database executed on the Qiita platform (Gonzalez et al., 2018) using default pipeline settings.

353 To discern patterns and significant differences in GMB, we employed global beta diversity
354 analysis using Jensen Shannon divergence (JSD) (Fuglede and Topsoe, 2004) as the distance
355 metric. JSD was selected because it was specifically determined to be highly effective for
356 generalizability and direct utility in biomedical contexts (Sáez et al., 2017). Statistical
357 significance of beta diversity measured using JSD was assessed by PERMANOVA (Anderson,
358 2014), using the vegan (Oksanen et al., 2007) package in R (Team, 2013). Specific
359 strain/species markers were identified using ANCOM-BC (Lin and Peddada, 2020) for all
360 outcomes (i.e. recurrence), with adjustment for age, sex, tumor stage, BRAF mutation and study
361 arm.

362 Given the regional disparities in GMB compositions, a meta-analysis was deemed
363 necessary. This was conducted on the identified region-specific markers to determine their
364 overarching association with recurrence across all regions. Meta analysis was performed using
365 the ANCOM-BC derived effect estimates and analyzed for pooled effect using the meta package
366 in R using random effect meta-analysis (Schwarzer, 2007), employing the default settings (Van
367 den Noortgate et al., 2013).

368 In the GMB matched analysis samples were selected on the basis of JSD similarity to
369 participants from the each discovery region (always selecting replication to include samples
370 outside of the discovery region). Specifically non-discovery region participants were checked for
371 JSD distance against all participants from the discovery region starting at JSD 0.01 (i.e. high
372 GMB similarity) and finishing at JSD 0.3 (i.e. low GMB similarity) with steps of 0.001. For a
373 replication participant to enter an analysis at a given JSD threshold, they need to have a match
374 to at least one discovery region patient with a JSD distance being equal to or lower than the
375 defined threshold. For example at the 0.11 JSD threshold, roughly the level of patient to self
376 distance, a participant would enter into the analysis if at least one discovery region subject has
377 a JSD of 0.11 or lower to him (indicating high GMB similarity) and discarded if no such match
378 could be made. Area under the curve analysis was performed using the pROC (Robin et al.,
379 2014) package in R.

380 For the comparison between beta diversity metrics and recurrence prediction, we
381 standardized metrics by setting the lower limit to the median intra-sample distance and the
382 upper limit to the median inter-sample distance, with 200 equal intervals in between the bounds
383 for testing AUC predicting on matched samples. This process of modeling for each involved
384 selecting non-North American patients for testing using North American regional markers based
385 on a beta-diversity threshold (each of the 200 steps), followed by AUC calculation in
386 independent testing set.

387

388 **Outcome Measures**

389 The primary outcome measure was the recurrence of melanoma post-treatment. Secondary
390 outcomes included regional variations in these associations and stability of the GMB during the
391 course of ICB treatment.

392

393 **Data Availability**

394 The raw sequence data for all baseline samples along with uncontrolled phenotype
395 variables reported in this paper have been deposited in the Genome Sequence Archive (Genomics,
396 Proteomics & Bioinformatics 2021) in National Genomics Data Center (Nucleic Acids Res 2021),
397 China National Center for Bioinformation / Beijing Institute of Genomics, Chinese Academy of
398 Sciences (GSA: HRA005933, direct link: <https://bigd.big.ac.cn/gsa-human/browse/HRA005933>) that
399 are publicly accessible at <https://ngdc.cncb.ac.cn/gsa>.

400 Additionally, all shotgun metagenomics sequencing data and the generated biom files
401 containing bacterial taxa and functional profiles are available within Qiita under the StudyID
402 13059.

403 **Acknowledgements**

404 We thank all of the participants of the Checkmate 915 trial (ID: NCT02388906) for providing
405 their samples and making this research possible. This publication includes data generated at
406 the UC San Diego IGM Genomics Center utilizing an Illumina NovaSeq 6000 that was
407 purchased with funding from a National Institutes of Health SIG grant (#S10 OD026929).
408 Research reported in this publication was supported in part by the U.S. National Cancer Institute
409 under award numbers P50 CA225450, P20CA252728, P30CA016087, R01CA159036,
410 R01LM014085-01A1, and U01CA250186.

411 **References:**

- 412
- 413 Anderson, M.J. (2014). Permutational multivariate analysis of variance (PERMANOVA). Wiley
- 414 statsref: statistics reference online, 1-15.
- 415 Araj, G., Maamari, J., Ahmad, F.A., Zareef, R., Chaftari, P., and Yeung, S.-C.J. (2022). The
- 416 emerging role of the gut microbiome in the cancer response to immune checkpoint inhibitors: a
- 417 narrative review. *Journal of Immunotherapy and Precision Oncology* 5, 13-25.
- 418 Baruch, E.N., Youngster, I., Ben-Betzalel, G., Ortenberg, R., Lahat, A., Katz, L., Adler, K., Dick-
- 419 Necula, D., Raskin, S., and Bloch, N. (2021). Fecal microbiota transplant promotes response in
- 420 immunotherapy-refractory melanoma patients. *Science* 371, 602-609.
- 421 Chen, L., Wang, D., Garmaeva, S., Kurilshikov, A., Vila, A.V., Gacesa, R., Sinha, T., Segal, E.,
- 422 Weersma, R.K., and Wijmenga, C. (2021). The long-term genetic stability and individual
- 423 specificity of the human gut microbiome. *Cell* 184, 2302-2315. e2312.
- 424 Cullin, N., Antunes, C.A., Straussman, R., Stein-Thoeringer, C.K., and Elinav, E. (2021).
- 425 Microbiome and cancer. *Cancer Cell* 39, 1317-1341.
- 426 Davar, D., Dzutsev, A.K., McCulloch, J.A., Rodrigues, R.R., Chauvin, J.-M., Morrison, R.M.,
- 427 Deblasio, R.N., Menna, C., Ding, Q., and Pagliano, O. (2021). Fecal microbiota transplant
- 428 overcomes resistance to anti-PD-1 therapy in melanoma patients. *Science* 371, 595-602.
- 429 Derosa, L., and Zitvogel, L. (2021). Fecal microbiota transplantation: can it circumvent
- 430 resistance to PD-1 blockade in melanoma? *Signal Transduction and Targeted Therapy* 6, 178.
- 431 Fuglede, B., and Topsoe, F. (2004). Jensen-Shannon divergence and Hilbert space embedding.
- 432 Paper presented at: International symposium on Information theory, 2004 ISIT 2004
- 433 Proceedings (IEEE).
- 434 Glenn, T.C., Nilsen, R.A., Kieran, T.J., Sanders, J.G., Bayona-Vásquez, N.J., Finger, J.W.,
- 435 Pierson, T.W., Bentley, K.E., Hoffberg, S.L., and Louha, S. (2019). Adapterama I: universal
- 436 stubs and primers for 384 unique dual-indexed or 147,456 combinatorially-indexed Illumina
- 437 libraries (iTru & iNext). *PeerJ* 7, e7755.
- 438 Gonzalez, A., Navas-Molina, J.A., Kosciolk, T., McDonald, D., Vázquez-Baeza, Y.,
- 439 Ackermann, G., DeReus, J., Janssen, S., Swafford, A.D., and Orchanian, S.B. (2018). Qiita:
- 440 rapid, web-enabled microbiome meta-analysis. *Nature methods* 15, 796-798.

- 441 Gopalakrishnan, V., Spencer, C.N., Nezi, L., Reuben, A., Andrews, M., Karpinets, T., Prieto, P.,
442 Vicente, D., Hoffman, K., and Wei, S.C. (2018). Gut microbiome modulates response to anti-
443 PD-1 immunotherapy in melanoma patients. *Science* 359, 97-103.
- 444 He, Y., Wu, W., Zheng, H.-M., Li, P., McDonald, D., Sheng, H.-F., Chen, M.-X., Chen, Z.-H., Ji,
445 G.-Y., and Mujagond, P. (2018a). Regional variation limits applications of healthy gut
446 microbiome reference ranges and disease models. *Nature medicine* 24, 1532-1535.
- 447 He, Y., Wu, W., Zheng, H.-M., Li, P., McDonald, D., Sheng, H.-F., Chen, M.-X., Chen, Z.-H., Ji,
448 G.-Y., and Zheng, Z.-D.-X. (2018b). Regional variation limits applications of healthy gut
449 microbiome reference ranges and disease models. *Nature medicine* 24, 1532-1535.
- 450 Kaplan, R.C., Wang, Z., Usyk, M., Sotres-Alvarez, D., Daviglius, M.L., Schneiderman, N.,
451 Talavera, G.A., Gellman, M.D., Thyagarajan, B., and Moon, J.-Y. (2019). Gut microbiome
452 composition in the Hispanic Community Health Study/Study of Latinos is shaped by geographic
453 relocation, environmental factors, and obesity. *Genome biology* 20, 1-21.
- 454 Lee, K.A., Thomas, A.M., Bolte, L.A., Björk, J.R., de Ruijter, L.K., Armanini, F., Asnicar, F.,
455 Blanco-Miguez, A., Board, R., and Calbet-Llopart, N. (2022). Cross-cohort gut microbiome
456 associations with immune checkpoint inhibitor response in advanced melanoma. *Nature*
457 *Medicine* 28, 535-544.
- 458 Lin, H., and Peddada, S.D. (2020). Analysis of compositions of microbiomes with bias
459 correction. *Nature communications* 11, 3514.
- 460 Liu, N., Chen, L., Yan, M., Tao, Q., Wu, J., Chen, J., Chen, X., Zhang, W., and Peng, C. (2023).
461 *Eubacterium rectale* Improves the Efficacy of Anti-PD1 Immunotherapy in Melanoma via I-
462 Serine-Mediated NK Cell Activation. *Research* 6, 0127.
- 463 Matson, V., Fessler, J., Bao, R., Chongsuwat, T., Zha, Y., Alegre, M.-L., Luke, J.J., and
464 Gajewski, T.F. (2018). The commensal microbiome is associated with anti-PD-1 efficacy in
465 metastatic melanoma patients. *Science* 359, 104-108.
- 466 McQuade, J.L., Ologun, G.O., Arora, R., and Wargo, J.A. (2020). Gut microbiome modulation
467 via fecal microbiota transplant to augment immunotherapy in patients with melanoma or other
468 cancers. *Current oncology reports* 22, 1-9.
- 469 Oksanen, J., Kindt, R., Legendre, P., O'Hara, B., Stevens, M.H.H., Oksanen, M.J., and
470 Suggests, M. (2007). The vegan package. *Community ecology package* 10, 719.

- 471 Olsson, L.M., Boulund, F., Nilsson, S., Khan, M.T., Gummesson, A., Fagerberg, L., Engstrand,
472 L., Perkins, R., Uhlen, M., and Bergström, G. (2022). Dynamics of the normal gut microbiota: A
473 longitudinal one-year population study in Sweden. *Cell Host & Microbe* 30, 726-739. e723.
- 474 Peters, B.A., Wilson, M., Moran, U., Pavlick, A., Izsak, A., Wechter, T., Weber, J.S., Osman, I.,
475 and Ahn, J. (2019). Relating the gut metagenome and metatranscriptome to immunotherapy
476 responses in melanoma patients. *Genome medicine* 11, 61.
- 477 Peters, B.A., Yi, S.S., Beasley, J.M., Cobbs, E.N., Choi, H.S., Beggs, D.B., Hayes, R.B., and
478 Ahn, J. (2020). US nativity and dietary acculturation impact the gut microbiome in a diverse US
479 population. *The ISME Journal* 14, 1639-1650.
- 480 Robin, X., Turck, N., Hainard, A., Tiberti, N., Lisacek, F., Sanchez, J.-C., Müller, M., Siegert, S.,
481 Doering, M., and Billings, Z. (2014). Package 'pROC' (Technical Report. Available online:
482 [https://cran.r-project.org/web ...](https://cran.r-project.org/web...)).
- 483 Routy, B., Le Chatelier, E., Derosa, L., Duong, C.P., Alou, M.T., Daillère, R., Fluckiger, A.,
484 Messaoudene, M., Rauber, C., and Roberti, M.P. (2018). Gut microbiome influences efficacy of
485 PD-1–based immunotherapy against epithelial tumors. *Science* 359, 91-97.
- 486 Sáez, C., Robles, M., and García-Gómez, J.M. (2017). Stability metrics for multi-source
487 biomedical data based on simplicial projections from probability distribution distances. *Statistical*
488 *methods in medical research* 26, 312-336.
- 489 Schwarzer, G. (2007). meta: An R package for meta-analysis. *R news* 7, 40-45.
- 490 Shim, J.A., Ryu, J.H., Jo, Y., and Hong, C. (2023). The role of gut microbiota in T cell immunity
491 and immune mediated disorders. *International Journal of Biological Sciences* 19, 1178.
- 492 Siegel, R.L., Miller, K.D., Wagle, N.S., and Jemal, A. (2023). Cancer statistics, 2023. *Ca Cancer*
493 *J Clin* 73, 17-48.
- 494 Simpson, R.C., Shanahan, E.R., Batten, M., Reijers, I.L., Read, M., Silva, I.P., Versluis, J.M.,
495 Ribeiro, R., Angelatos, A.S., and Tan, J. (2022). Diet-driven microbial ecology underpins
496 associations between cancer immunotherapy outcomes and the gut microbiome. *Nature*
497 *medicine* 28, 2344-2352.
- 498 Spencer, C.N., McQuade, J.L., Gopalakrishnan, V., McCulloch, J.A., Vetizou, M., Cogdill, A.P.,
499 Khan, M.A.W., Zhang, X., White, M.G., and Peterson, C.B. (2021). Dietary fiber and probiotics
500 influence the gut microbiome and melanoma immunotherapy response. *Science* 374, 1632-
501 1640.

- 502 Team, R.C. (2013). R: A language and environment for statistical computing.
- 503 Thompson, L.R., Sanders, J.G., McDonald, D., Amir, A., Ladau, J., Locey, K.J., Prill, R.J.,
504 Tripathi, A., Gibbons, S.M., and Ackermann, G. (2017). A communal catalogue reveals Earth's
505 multiscale microbial diversity. *Nature* 551, 457-463.
- 506 Usyk, M., Peters, B.A., Karthikeyan, S., McDonald, D., Sollecito, C.C., Vazquez-Baeza, Y.,
507 Shaffer, J.P., Gellman, M.D., Talavera, G.A., and Daviglus, M.L. (2023). Comprehensive
508 evaluation of shotgun metagenomics, amplicon sequencing, and harmonization of these
509 platforms for epidemiological studies. *Cell Reports Methods* 3.
- 510 Van den Noortgate, W., López-López, J.A., Marín-Martínez, F., and Sánchez-Meca, J. (2013).
511 Three-level meta-analysis of dependent effect sizes. *Behavior research methods* 45, 576-594.
- 512 Vangay, P., Johnson, A.J., Ward, T.L., Al-Ghalith, G.A., Shields-Cutler, R.R., Hillmann, B.M.,
513 Lucas, S.K., Beura, L.K., Thompson, E.A., and Till, L.M. (2018). US immigration westernizes the
514 human gut microbiome. *Cell* 175, 962-972. e910.
- 515 Weber, J.S., Schadendorf, D., Del Vecchio, M., Larkin, J., Atkinson, V., Schenker, M., Pigozzo,
516 J., Gogas, H., Dalle, S., and Meyer, N. (2023). Adjuvant therapy of nivolumab combined with
517 ipilimumab versus nivolumab alone in patients with resected stage IIIB-D or stage IV melanoma
518 (CheckMate 915). *Journal of Clinical Oncology* 41, 517.
519
520

Table 1. Demographic and Clinical Characteristics of Study Participants, Stratified by Geographic Region

Variable	Overall	North America*	Australia	Western Europe	Eastern Europe	ROW**
N	674	95	127	367	43	42
Age Mean ± SD	55.03 ± 13.88	55.29 ± 14.26	55.31 ± 13.73	54.72 ± 13.73	51.77 ± 15.17	58.9 ± 12.68
Gender						
Female	277 (41.1%)	40 (42.1%)	44 (34.6%)	160 (43.6%)	19 (44.2%)	14 (33.3%)
Male	397 (58.9%)	55 (57.9%)	83 (65.4%)	207 (56.4%)	24 (55.8%)	28 (66.7%)
Race						
White	667 (99.0)	91 (95.8%)	126 (99.2%)	366 (99.7%)	43 (100%)	41 (97.6%)
Other	7 (1.0%)	4 (4.2%)	1 (0.8%)	1 (0.3%)	0 (0%)	1 (2.4%)
Recurrence						
Yes	252 (37.4%)	32 (33.7%)	49 (38.6%)	137 (37.3%)	24 (55.8%)	10 (23.8%)
No	422 (67.6%)	63 (66.3%)	78 (61.4%)	230 (62.7%)	19 (44.2%)	32 (76.2%)
Median Follow-up Time (months) ± IQR	24.9 ± 19.8	23.4 ± 17.5	24.9 ± 22.1	24.8 ± 19.7	15.0 ± 25.7	27.6 ± 3.0
Trial Arm						
Nivo240mg+Ipi1mg/kg	346 (51.3%)	45 (47.4%)	62 (48.8%)	190 (51.8%)	25 (58.1%)	24 (57.1%)
Nivolumab 480mg	328 (48.7%)	50 (52.6%)	65 (51.2%)	177 (48.2%)	18 (41.9%)	18 (42.9%)
Stage						
IIIB	201 (29.8%)	29 (30.5%)	39 (30.7%)	113 (30.8%)	11 (25.6%)	9 (21.4%)
IIIC	366 (54.3%)	57 (60%)	62 (48.8%)	199 (54.2%)	26 (60.5%)	22 (52.4%)
IIID	15 (2.2%)	4 (4.2%)	1 (0.8%)	9 (2.5%)	0 (0%)	1 (2.4%)
IV	92 (13.7%)	5 (5.3%)	25 (19.7%)	46 (12.5%)	6 (14%)	10 (23.8%)
BRAF Mutation						
Wildtype	325 (48.2%)	47 (49.5%)	67 (52.8%)	182 (49.6%)	19 (44.2%)	10 (23.8%)
Mutant	188 (27.9%)	20 (21.1%)	35 (27.6%)	111 (30.2%)	19 (44.2%)	3 (7.1%)
Missing	161 (23.9%)	28 (29.5%)	25 (19.7%)	74 (20.2%)	5 (11.6%)	29 (69%)
LD*** (L/U, mean ± SD)	216.6 ± 86.5	186.8 ± 84.3	189.7 ± 3	230.5 ± 93.3	187.4 ± 52.3	276.8 ± 109.5
Missing (N)	12	0	1	9	1	1

* North America (NA: U.S. and Canada); ** ROW stands for “rest of world”, patients from Brazil (n = 28) and New Zealand (n = 14).

*** LD refers lactate dehydrogenase (LDH) level and L/U represent the Lower/Upper of the test result

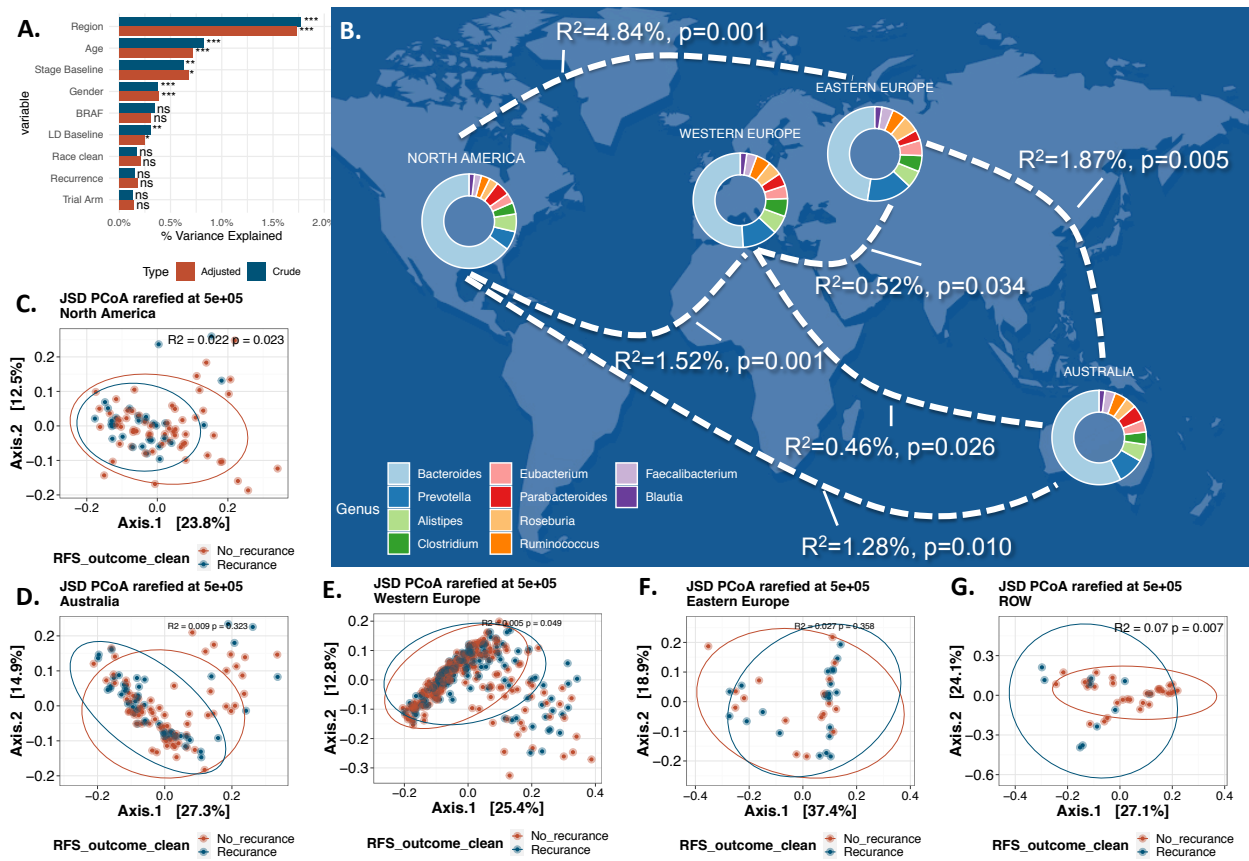


Figure 1. Beta Diversity, Regional Variation and Melanoma Recurrence

(A) illustrates a PERMANOVA analysis of essential clinical and demographic variables within our study, using JSD distance. Color indicates the analysis type: crude in blue and adjusted (adjustment for each other variable) in orange. The x-axis denotes R^2 , reflecting the proportion of overall gut microbiota composition variance, with stars adjacent to the bars indicating significance (p-values: 0.05 *, 0.01 **, 0.001 ***, >0.05 NS). Panel (B) presents a map of the geographic regions, with paired PERMANOVA results for each geographic pair displayed on the plotted curves. All pairs exhibited significant differences. Donut charts plotted over each geographic region represent the top 10 genera across (based on abundance) all samples within that region. Panels (C-G) depict the principal coordinate analysis (PCoA) for each of the five geographic regions, considering recurrence as the outcome (R^2 and p-values are provided for each region).

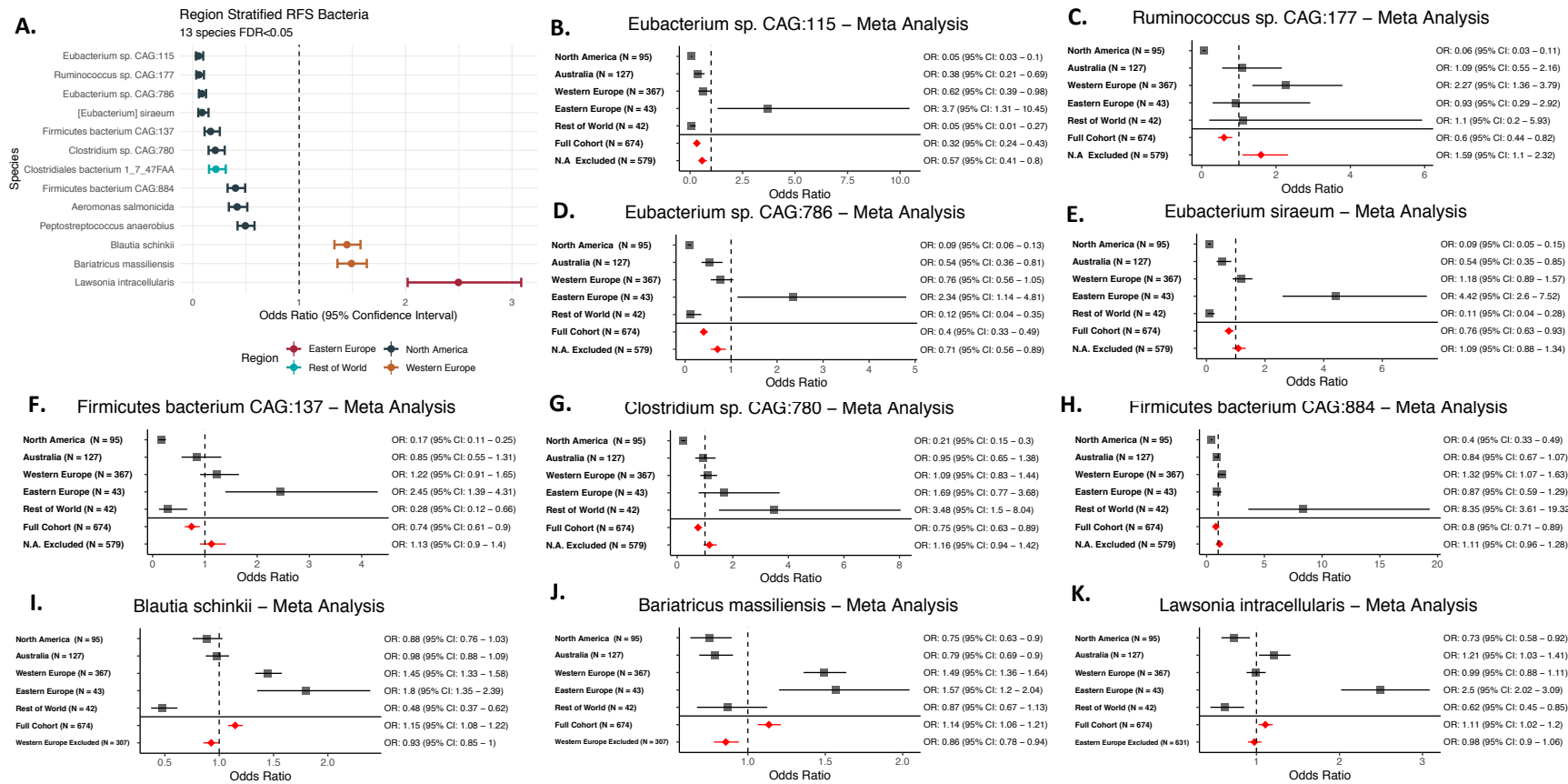


Figure 2. Region Stratified Analysis of Individual GMB Taxa and Melanoma Recurrence

(A) shows the region-stratified analysis as a forest plot with each point and associated confidence interval colored by the geographic region in which the identified gut microbiome markers prospectively associated with melanoma recurrence. All strains shown are significant after adjustment for multiple testing (FDR<0.05), with effects adjusted for participant age, sex, tumor stage, BRAF mutation and study arm.

(B-K) show the meta-analysis of region-specific gut microbiome markers associated with recurrence in melanoma patients across geographic regions. Each panel shows analysis of a specific microbiome strain by region and, in meta-analyses, for the full cohort and for the full cohort minus the discovery region in (A) (N.A. stands for North America in the exclusion line). Meta analyses were performed using random-effect meta-analysis models (Schwarzer, 2007). Bacteria from (A) that are not significant in meta-analysis (*Aeromonas salmonicida*, *Clostridiales bacterium 1-7-47 FAA* and *Peptostreptococcus anaerobius*) are not shown in (B-K).



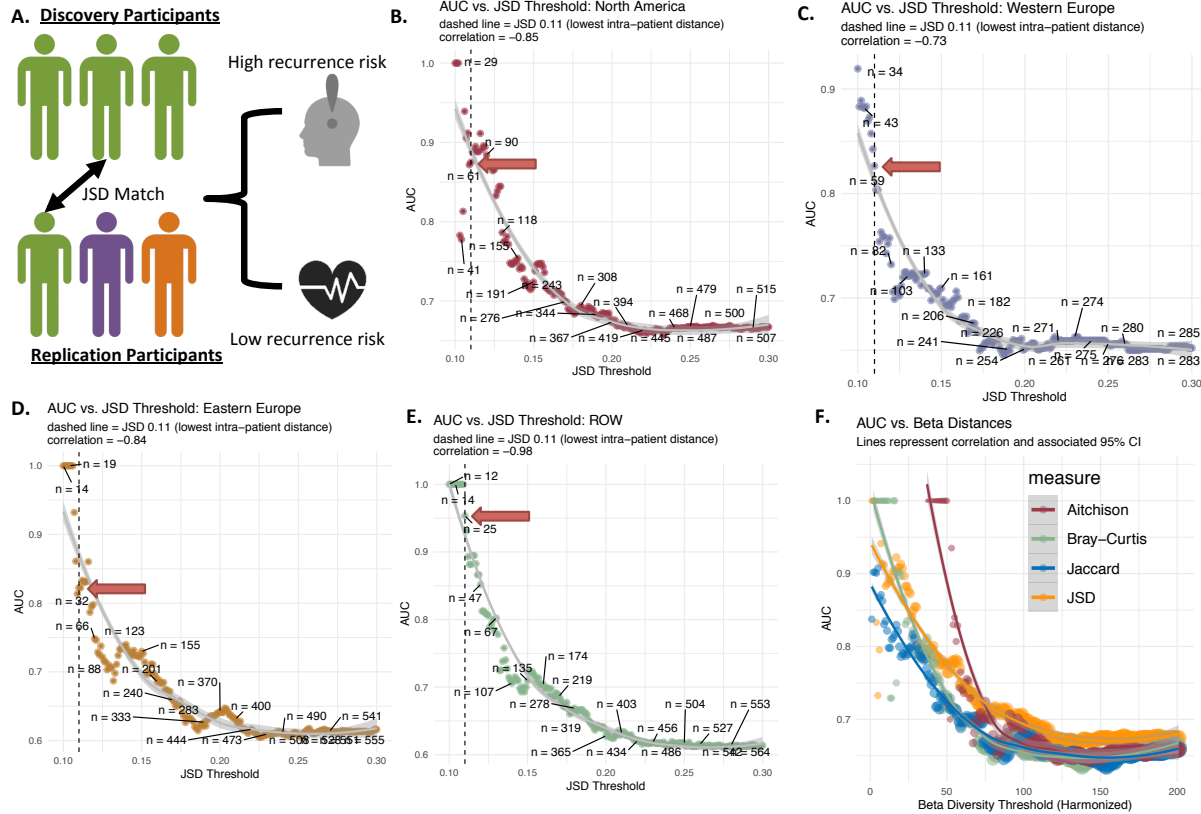


Figure 4. Recurrence Risk Prediction Models in Patients Using Independent Cross-regional Replicates Matched on GMB

Panel A depicts the patient matching method employed to generalize markers (i.e. using the region specific markers in other geographic areas for patients with the “same” GMB). JSD was used to match patients across region (testing patients are always from a different region from training patients), and subsequently, the predictive power of biomarkers was evaluated in the subsequent panels with adjustment for age, sex, tumor stage, BRAF mutation and study arm. **Panel B** shows the relationship between prediction measured using AUC vs. increasing JSD distance (spearman correlation = -0.85 , $p < 0.001$). For each point (200 total) a non-North American patient is matched to a North American subject at each JSD threshold and the final independently matched set is modeled using the North America markers to obtain AUC. **Panel C, D and E** show the same analysis, but using the ROW, Eastern Europe and Western Europe as discovery sets respectively. **Panel F** shows the comparison between the original JSD beta-diversity as well as Bray-Curtis dissimilarity, Jaccard index, and Aitchison dissimilarity with respect to AUC predictive power. Metrics were standardized by setting the lower limit to the median intra-sample distance and the upper limit to the median inter-sample distance, with 200 equal intervals for testing.

GMB Stability Across Time

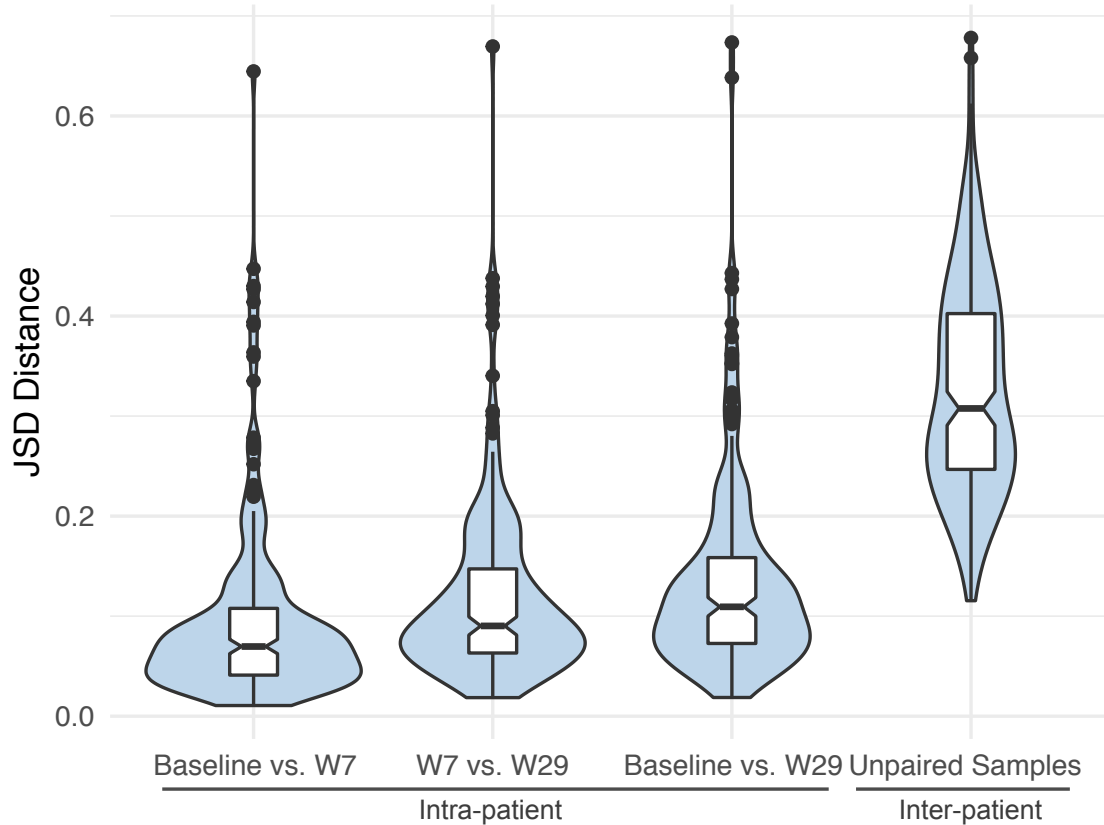


Figure 5. GMB Stability Across Time

Figure shows the bacterial β -diversity measured using Jensen Shannon divergence between measured visits (intra-patient variation) as well as between all unpaired samples for reference (inter-patient variation). Overall GMB was largely unchanged across baseline, week 7 and week 29 measurements with global PERMANOVA $R^2 = 0.867$, $p\text{-val} < 0.001$. Comparison between baseline and week 7 samples had an $R^2 = 0.930$, $p\text{-val} < 0.001$; week 7 vs. week 29 $R^2 = 0.900$, $p\text{-val} < 0.001$.

Supplement Table of Contents

Tables

Supplemental Table 1. Region Stratified ANCOM-BC Results

Figures

Supplemental Figure 1. Study Consort Chart

Supplemental Figure 2. JSD Distances Across Time, Stratified by Trial Arm

Supplemental Figure 3. JSD Distances Across Time, Stratified by Recurrence Status

Supplemental Figure 4. PCOA Plot by Time Points

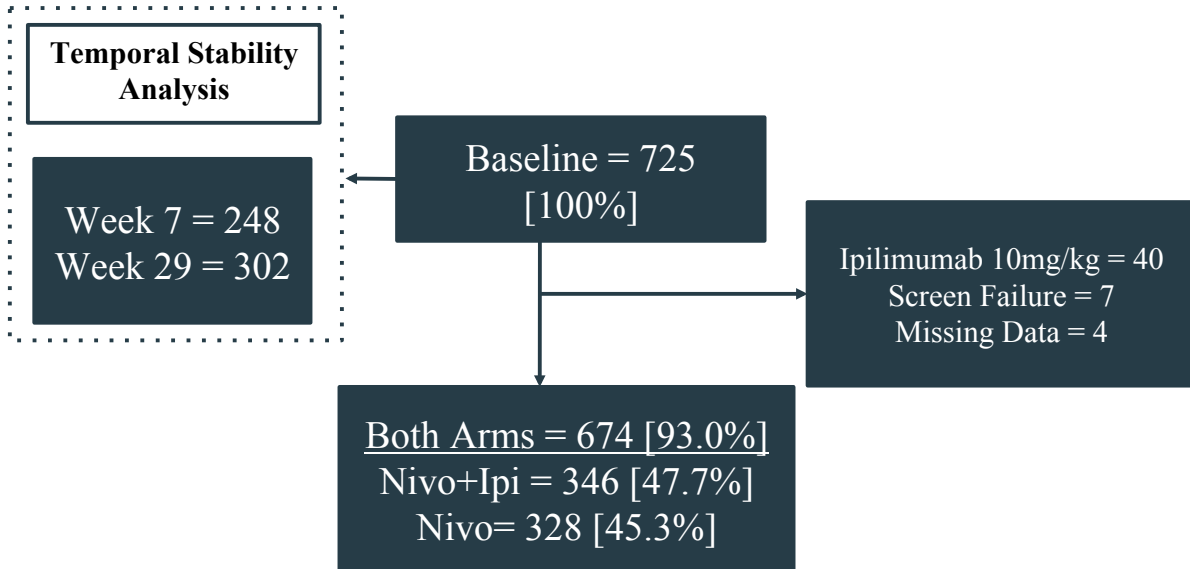
Supplemental Table 1. Region Stratified ANCOM-BC Results

Region	Recurrence Associated Strain	OR	95% CI, low	95% CI, high	p-val	q-val
North America	Firmicutes bacterium CAG:137	0.17	0.25	0.11	1.64E-05	0.028
North America	Firmicutes bacterium CAG:884	0.40	0.49	0.33	8.43E-06	0.015
North America	Clostridium sp. CAG:780	0.21	0.30	0.15	9.26E-06	0.016
North America	Eubacterium sp. CAG:115	0.054	0.10	0.030	9.76E-07	0.0017
North America	Eubacterium sp. CAG:786	0.09	0.13	0.058	1.67E-10	2.89E-07
North America	Peptostreptococcus anaerobius	0.49	0.58	0.42	1.13E-05	0.020
North America	Eubacterium siraeum	0.088	0.15	0.052	3.39E-06	0.006
North America	Ruminococcus sp. CAG:177	0.059	0.11	0.033	9.74E-07	0.0017
North America	Aeromonas salmonicida	0.42	0.51	0.34	2.37E-05	0.041
Western Europe	Bariatricus massiliensis	1.49	1.64	1.36	1.50E-05	0.028
Western Europe	Blautia schinkii	1.45	1.58	1.33	1.13E-05	0.021
Eastern Europe	Lawsonia intracellularis	2.50	3.09	2.02	1.62E-05	0.030
Rest of World	Clostridiales bacterium 1_7_47FAA	0.22	0.31	0.15	1.60E-05	0.032

Table shows the results of ANCOM-BC analysis of recurrence as the outcome with GMB as the core predictor with adjustment for participant age, sex, tumor stage, BRAF mutation and study arm. Odds ratios (ORs) are shown with associated p-values as well as adjusted values using the “holm” method.

Supplemental Table 2: Patients with Longitudinal Sampling

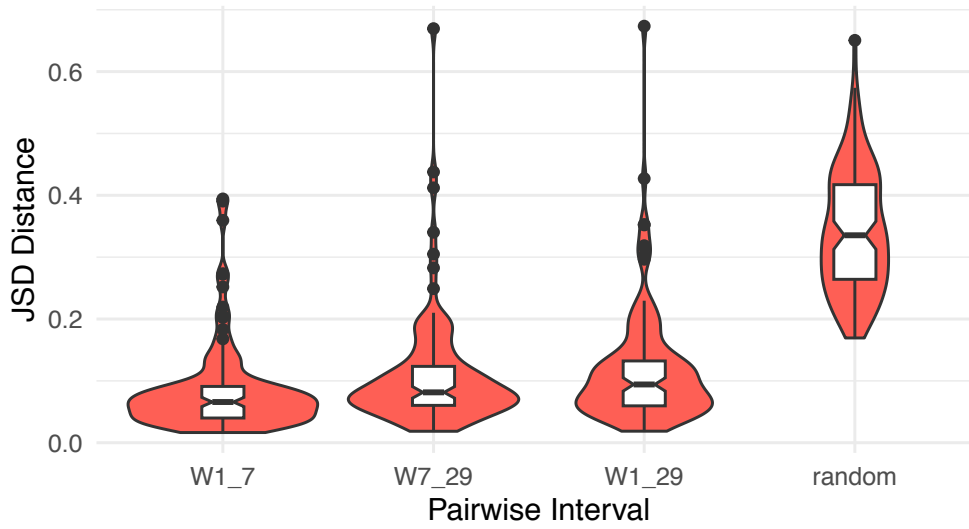
Variable	No	Yes	OR	pval
N	424	301		
Recurrence				
No	228 (55.2%)	219 (72.8%)	0.46 (0.33 - 0.64)	1.68E-06
Yes	185 (44.8%)	82 (27.2%)	-	-
Missing (n = 11)				
Age Mean± SD	54.54± 14.32	55.4± 13.3	-	0.685
Gender				
Female	178 (42.4%)	120 (39.9%)	1.11 (0.81 - 1.52)	0.54
Male	242 (57.6%)	181 (60.1%)	-	-
Missing (n = 4)				
Region				
Australia	77 (18.2%)	64 (21.3%)	-	0.13
Eastern Europe	24 (5.7%)	21 (7%)	-	0.125
ROW	29 (6.8%)	19 (6.3%)	-	0.284
North America	66 (15.6%)	39 (13%)	-	0.295
Western Europe	224 (52.8%)	158 (52.5%)	-	0.148
Stage at entry				
Not Reported	7 (1.7%)	0 (0%)	-	1
Stage IIIB	113 (26.7%)	102 (33.9%)	-	0.125
Stage IIIC	234 (55.2%)	152 (50.5%)	-	0.16
Stage IIID	10 (2.4%)	5 (1.7%)	-	0.53
Stage IV	56 (13.2%)	42 (14%)	-	0.141
B.Raf.Mut				
Invalid/Not Reported	104 (24.5%)	75 (24.9%)	-	0.145
Mutant	119 (28.1%)	79 (26.2%)	-	0.157
Wildtype	197 (46.5%)	147 (48.8%)	-	0.141
Melanoma Subtypes				
Acral	14 (3.3%)	9 (3%)	-	0.268
Cutaneous	357 (84.2%)	264 (87.7%)	-	0.142
Mucosal	4 (0.9%)	1 (0.3%)	-	1
Not Reported	8 (1.9%)	0 (0%)	-	1
Other	37 (8.7%)	27 (9%)	-	0.146
LD_baseline Mean± SD	218.92± 85.25	213.48± 88.16	-	0.207



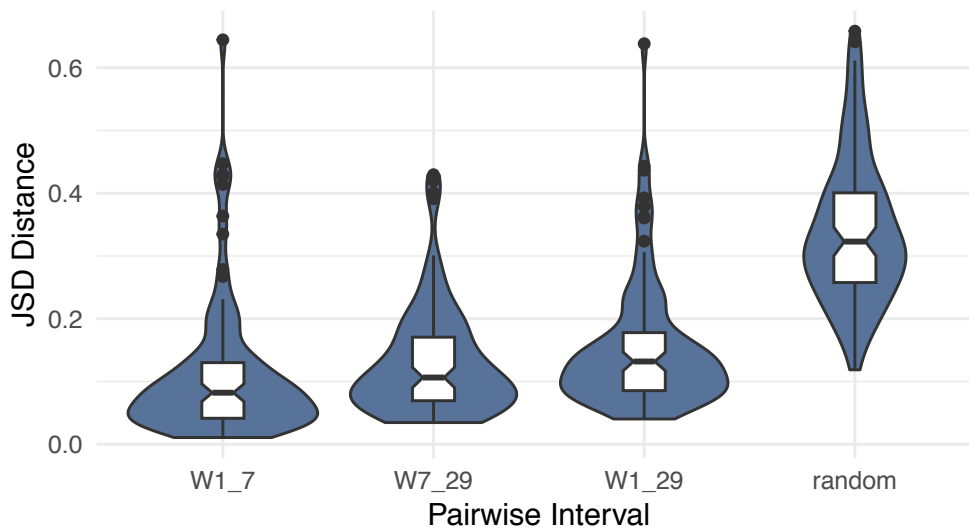
Supplemental Figure 1. Study Consort Chart

725 represented baseline. Of these, approximately half of the patients had follow-up sampling at weeks 7 and 29. From the baseline samples, 51 individuals were excluded due to coming from a supplementary arm of the original trial (n = 40), being screen failures (n = 7) or having missing randomization data (n = 4). Overall we utilized 674/725 (93.0%) of the available shotgun metagenomic samples for our core analysis.

A. GMB Stability: Nivolumab 480mg

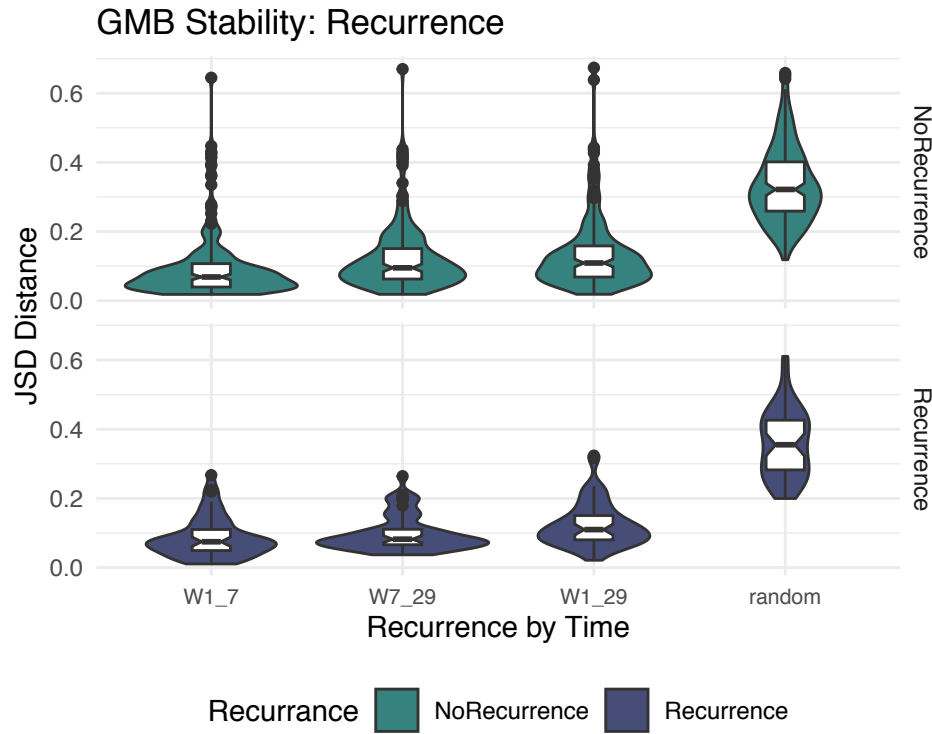


B. GMB Stability: Nivo240mg+Ipi1mg/kg



Supplemental Figure 2. JSD Distances Across Time, Stratified by Trial Arm

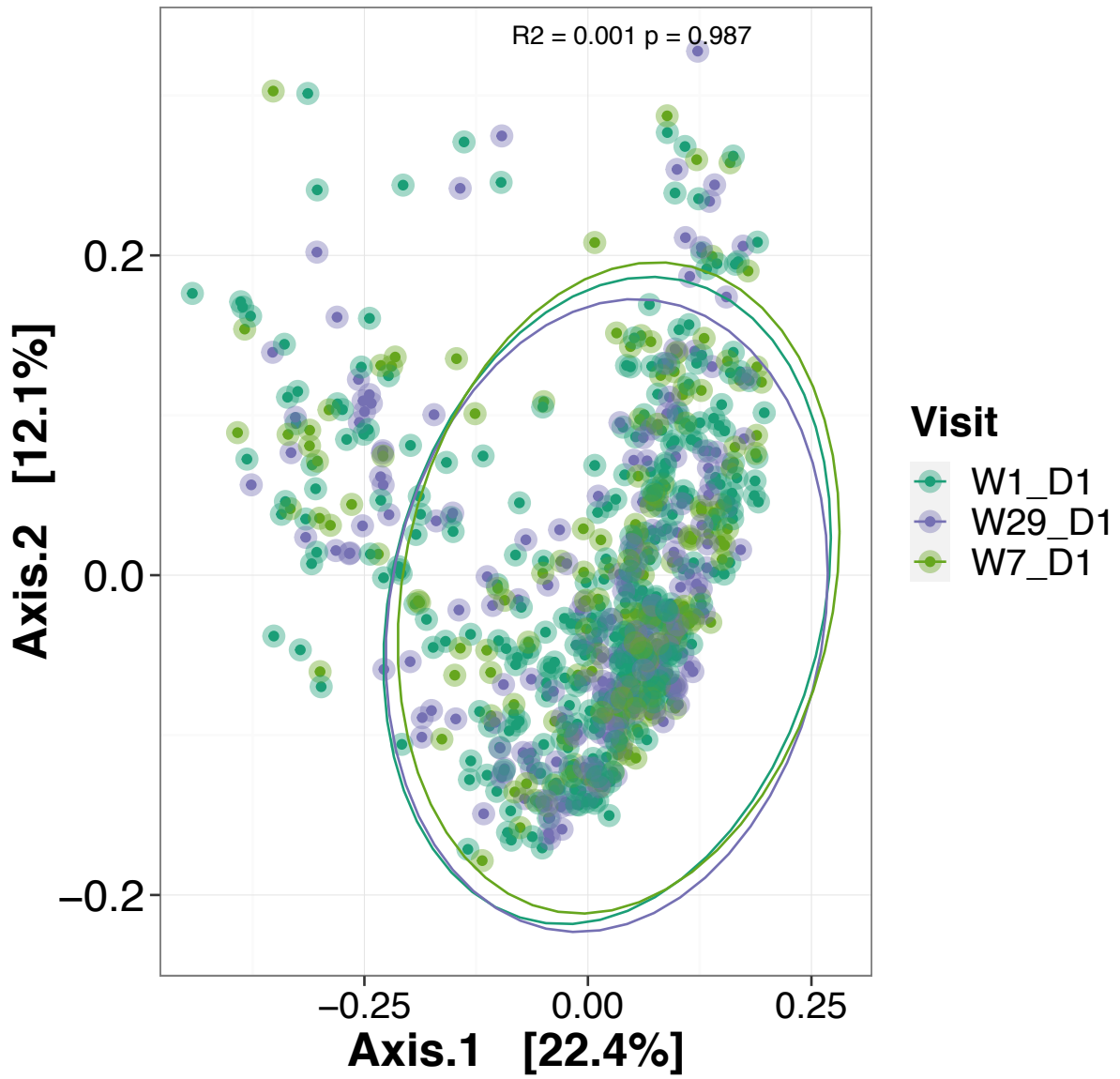
The figure shows the bacterial β -diversity measured using Jensen Shannon divergence between measured visits (intra-patient variation) as well as between all unpaired samples for reference (inter-patient variation), stratified by the treatment arm (red, panel A is mono treatment and blue panel B is combination treatment). Overall GMB was largely unchanged across baseline, week 7 and week 29 measurements in both arms.



Supplemental Figure 3. JSD Distances Across Time, Stratified by Recurrence Status

The figure shows the bacterial β -diversity measured using Jensen Shannon divergence between measured visits (intra-patient variation) as well as between all unpaired samples for reference (inter-patient variation), stratified by recurrence status (green, panel A: no recurrence group and navy, panel B, recurrence group). Overall GMB was largely unchanged across baseline, week 7 and week 29 measurements in both panels.

PCoA jsd rarefied at 5e+05



Supplemental Figure 3. PCOA plot by Time Points

PCOA plot for three-time points as the outcome for the BMS patients using JSD distances.